The Meridional Variation of the Eddy Heat Fluxes by Baroclinic Waves and Their Parameterization

PETER H. STONE

Institute for Space Studies, Goddard Space Flight Center, NASA, New York, N. Y. 10025 and Dept. of Meteorology, Massachusetts Institute of Technology, Cambridge 02139

(Manuscript received 10 September 1973)

ABSTRACT

The meridional and vertical eddy fluxes of sensible heat produced by small-amplitude growing baroclinic waves are calculated using solutions to the two-level model with horizontal shear in the mean flow. The results show that the fluxes are primarily dependent on the local baroclinicity, i.e., the local value of the isentropic slopes in the mean state. Where the slope exceeds the critical value, the transports are poleward and upward; where the slope is less than the critical value, the transports are equatorward and downward.

These results are used to improve an earlier parameterization of the tropospheric eddy fluxes of sensible heat based on Eady's model. Comparisons with observations show that the improved parameterization reproduces the observed magnitude and sign of the eddy fluxes and their vertical variations and seasonal changes, but the maximum in the poleward flux is too near the equator. The corresponding parameterizations for the eddy coefficients describing the transport of any conserved quantity are given.

1. Introduction

One of the most important properties of baroclinic waves is their transport of heat poleward and upward. Observational studies show that these transports account for a substantial part of the atmosphere's total heat transport (Palmén and Newton, 1969, Chap. 2) and theoretical studies show that they are of crucial importance in determining the atmosphere's thermal structure (Stone, 1972). In addition, they help drive the mean meridional circulations (Kuo, 1956). Consequently, all models of the atmosphere must include these fluxes, and in particular one- and two-dimensional models must include them in parameterized form (Sellers, 1969; Kurihura, 1970; Wiin-Nielsen, 1970; Saltzman and Vernekar, 1971). In fact, Green (1970) has shown that a successful parameterization of the eddy heat flux by baroclinic waves is the key to the parameterization of many of the other large-scale eddy fluxes in the troposphere.

So far the work done on parameterizing these eddy heat fluxes has concentrated on determining how the mean flux depends on basic parameters such as the mean horizontal temperature gradient (Clapp, 1970; Green, 1970; Stone, 1972). However, accurate representations for the meridional variations of the eddy fluxes are also needed. One way to obtain useful information for parameterizing these meridional variations is to calculate the eddy fluxes rigorously from a realistic model of small-amplitude, growing baroclinic waves. In Sections 2–4 we present such a calculation. Section 2 contains a description of the model we use, and Sections 3 and 4 contain solutions for the meridional and vertical eddy fluxes, respectively. In Section 5 we use these solutions to derive an improved parameterization for the eddy fluxes and compare it with the observations.

2. The model

The details of the model we will use have already been described (Stone, 1969). This model is the simplest model of baroclinic instability which allows the meridional variations of the zonal wind to be included in a realistic way. It starts from Charney and Phillips' (1953) two-level model. The basic equation for the pressure perturbation due to the baroclinic wave in this model is the linearized form of the vorticity equation. In dimensional form this equation may be written as

$$(\bar{u}-c)\left(\frac{d^2\Pi_3}{dy^2}-k^2\Pi_3\right)+\left(b-\frac{d^2\bar{u}}{dy^2}+4\bar{u}\right)\Pi_3 = -4(\bar{u}-c)(\Pi_1-\Pi_3), \quad (2.1)$$

$$-c\left(\frac{d^2\Pi_1}{dy^2}-k^2\Pi_1\right)+(b-4\bar{u})\Pi_1=4c(\Pi_3-\Pi_1). \quad (2.2)$$

Subscripts 1 and 3 refer, respectively, to the lower and upper levels, Π is the pressure perturbation, $\bar{u}(y)$ the unperturbed zonal flow in the upper layer (the value in the lower layer being taken as zero), y the meridional coordinate, c the complex phase speed, and k the longitudinal wavenumber; b is a dimensionless param-

eter defined as

$$b=\frac{\beta L^2}{u_0}, \tag{2.3}$$

where $\beta=2\Omega\cos\phi/R$, Ω is the earth's rotation rate, ϕ the latitude, R the earth's radius, u_0 the magnitude of the unperturbed zonal flow in the upper layer, and L the radius of deformation (assumed to be constant) [$\bar{u}$ and c are measured in units of u_0, y in units of L, and k in units of $1/L$]. The boundary conditions are that the perturbation goes to zero at the equator and the pole, i.e.,

$$\Pi_3=\Pi_1=0 \quad \text{at} \quad y=\pm y_0\equiv\pm\frac{\pi}{4}\frac{R}{L}. \tag{2.4}$$

Eqs. (2.1) and (2.2) may be simplified by assuming that the scale of the unperturbed zonal flow is of order R and that

$$\epsilon\equiv\frac{1}{y_0}=\frac{4L}{\pi R}\ll 1. \tag{2.5}$$

This assumption allows the y-dependence of Eqs. (2.1) and (2.2) to be treated by "two-timing" techniques, with the two y-scales being L and R (see Stone, 1969). The solution to Eqs. (2.1) and (2.2), ignoring terms of order ϵ, is then

$$\Pi_3=\left[\frac{1}{\lambda(1+g^2)}\right]^{\frac{1}{2}}\sin\eta, \tag{2.6}$$

$$\Pi_1=g\Pi_3, \tag{2.7}$$

where

$$\lambda=\left\{\frac{1}{2}\frac{4\bar{u}(y)+b}{\bar{u}(y)-c}+\frac{1}{2}\frac{4\bar{u}(y)-b}{c}-k^2-4+\frac{1}{2}\left[\left(\frac{4\bar{u}(y)+b}{\bar{u}-c}-\frac{4\bar{u}-b}{c}\right)^2+64\right]^{\frac{1}{2}}\right\}^{\frac{1}{2}}, \tag{2.8}$$

$$g=1+\frac{k^2}{4}-\frac{4\bar{u}(y)+b}{4[\bar{u}(y)-c]}+\frac{\lambda^2}{4}, \tag{2.9}$$

$$\eta=\int_{-y_0}^{+y}\lambda(y)dy. \tag{2.10}$$

The eigenvalue c is the solution of the integral equation

$$\int_{-y_0}^{+y_0}\lambda(y,c,k,b)dy=m\pi, \tag{2.11}$$

where m is the meridional wavenumber. From these formulas one can explicitly calculate the eigenvalue and eigenfunctions for any $\bar{u}(y)$, ϵ, and $b\leqslant 3.5$, and determine which eigenvalue, as specified by k and m, has the largest growth rate. A number of such solutions for $4\leqslant b\leqslant 3.5$, i.e., near-neutral stability, have been described (Stone, 1969) and we will use these same solutions to calculate the heat fluxes that accompany the most rapidly growing modes.

For this purpose we need to relate the meridional and vertical velocities, v and w, respectively, and the potential temperature θ, to Π_1 and Π_3. The relevant linearized equations for the two-level model are given by Charney and Phillips (1953) and Phillips (1954). In dimensionless form they are

$$v_2=\tfrac{1}{2}ik(\Pi_1+\Pi_3), \tag{2.12}$$

$$\theta_2=2(\Pi_3-\Pi_1), \tag{2.13}$$

$$w_2=ik(c-\tfrac{1}{2}\bar{u})\theta+2\bar{u}v_2. \tag{2.14}$$

Here the subscript 2 refers to a level intermediate between levels 1 and 3. Eq. (2.12) follows from the assumption of geostrophic balance, (2.13) from hydrostatic equilibrium, and (2.14) from adiabatic motion. The zonally averaged meridional and vertical eddy fluxes of heat (actually of sensible heat plus potential energy) at level 2 are proportional to

$$\overline{\theta v}=\tfrac{1}{2}\,\mathrm{Re}\theta_2 v_2^*, \tag{2.15}$$

$$\overline{\theta w}=\tfrac{1}{2}\,\mathrm{Re}\theta_2 w_2^*. \tag{2.16}$$

Since the eddy flux of potential energy is small (Oort and Rasmusson, 1971), the θ fluxes are almost the same as the sensible heat fluxes, and we will refer to them as such. Substituting Eqs. (2.12) to (2.14) into (2.15) and (2.16), we obtain

$$\overline{\theta v}=k(\Pi_3\Pi_1^*)_i, \tag{2.17}$$

$$\overline{\theta w}=-2kc_i|\Pi_3-\Pi_1|^2+2\bar{u}\overline{\theta v}, \tag{2.18}$$

where an asterisk denotes the complex conjugate, the subscript i the imaginary part, and a bar the zonal average.

Phillips (1954) has discussed the solution of Eqs. (2.1) and (2.2) subject to boundary conditions (2.4) when there is no meridional shear in the unperturbed zonal flow, i.e., when $\bar{u}=1$. In this case both of the eddy transports are positive everywhere, their latitude dependence being given by $\{\sin(m\pi/2)[(y/y_0)+1]\}^2$ and $m=1$ for the most unstable mode. Also, we note that for any $\bar{u}(y)$, the two fluxes are proportional to each other if we are sufficiently near neutral stability, i.e.,

$$\overline{\theta w}=2\bar{u}\overline{\theta v}, \quad \text{when } c_i=0. \tag{2.19}$$

3. The meridional eddy heat flux

Figs. 1–7 illustrate $\overline{v\theta}$ calculated from Eq. (2.17) using the most unstable modes for different choices of $\bar{u}$ and b. [The eigenvalues and eigenfunctions may be found in

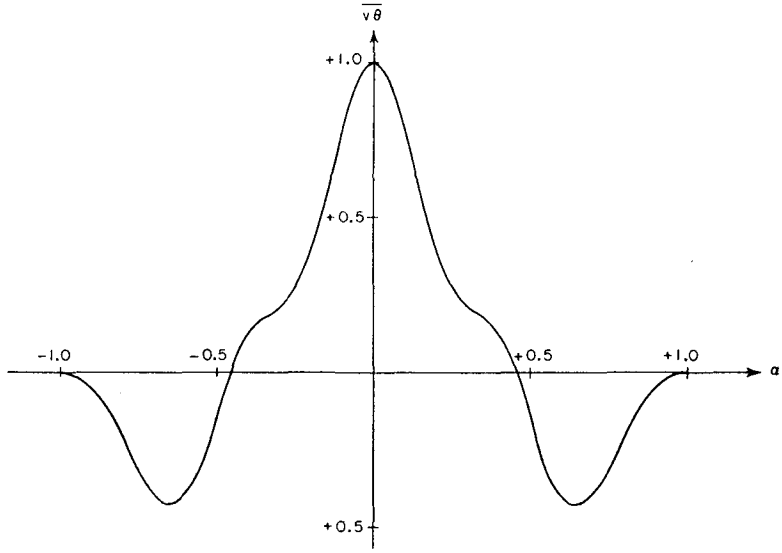

FIG. 1. Meridional heat transport vs latitude using the most unstable mode ($m=3$), for $b=3.8$, $\bar{u}=1-\frac{1}{4}\alpha^2$.

Section 4 of Stone (1969).] All the calculations are for $\epsilon\approx 0.2$, corresponding to $L\approx 1000$ km. For convenience in plotting the results a normalized independent variable,

$$\alpha=\frac{y}{y_0}, \tag{3.1}$$

has been used, and $\overline{v\theta}$ was normalized to its maximum value.

Figs. 1 and 2 show how $\overline{v\theta}$ depends on $\bar{u}(y)$. In Fig. 1, $\bar{u}=1-\frac{1}{4}\alpha^2$, $b=3.8$; in Fig. 2, $\bar{u}=1-\frac{1}{2}\alpha^2$, $b=3.8$. Comparing these figures with $\overline{v\theta}$ for the most unstable mode when $\bar{u}=1$ we see that the more concentrated the zonal jet is, the more concentrated the region of poleward heat transport near the center of the jet becomes, with the transport under the wings of the jet becoming equatorward.

For the case illustrated in Fig. 2 the mode $m=4$ was almost as unstable as the mode $m=3$. Fig. 2 shows $\overline{v\theta}$ for $m=3$, while Fig. 3 shows it for $m=4$. The regions of poleward and equatorward transport are virtually identical for the two modes. The transport does just go to zero at the center of the jet for $m=4$, as it would for any even mode. This property is an artifact of choosing $\bar{u}$ to be perfectly symmetric about $y=0$. For

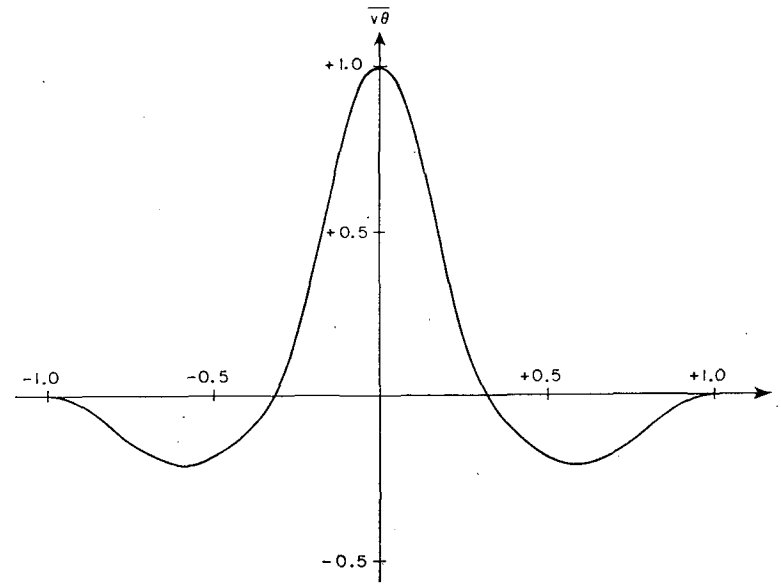

FIG. 2. As in Fig. 1, but for $\bar{u}=1-\frac{1}{2}\alpha^2$.

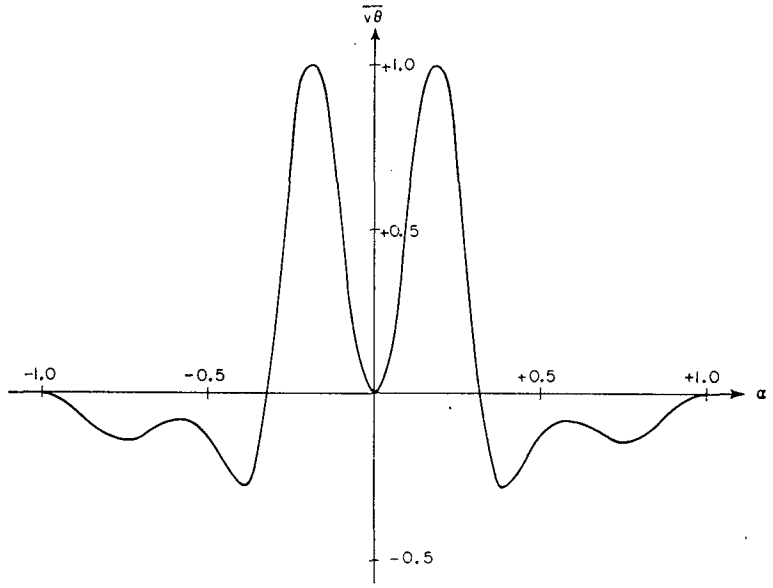

FIG. 3. As in Fig. 1, but for $\bar{u}=1-\frac{1}{2}\alpha^2$ and $m=4$.

any nonsymmetric jet the transport would be positive at the center of the jet.

Figs. 4–6 illustrate the dependence of $\overline{v\theta}$ on b (or equivalently u_0). In all three figures $\bar{u}=(1+\alpha^2)^{-1}$, and the values of b were 3.8, 3.65 and 3.5, respectively.

In the case $b=3.8$, the mode $m=4$ was slightly more unstable than the mode $m=3$, but the latter mode was used to compute $\overline{v\theta}$ in order to simplify the comparison with the other two cases where $m=3$ was the most unstable one. Figs. 4–6 show that the regions with poleward heat transport become larger as one moves away from neutral stability.

Fig. 7 illustrates $\overline{v\theta}$ when $\bar{u}$ consists of two jets, symmetric about $\alpha=0$, with maxima $\bar{u}(\pm\frac{1}{2})=1$, minima $\bar{u}(\pm 1)=0.75$, and $\bar{u}(0)=0.8$. [The detailed form of this in profile is given in Fig. 22 of Stone (1969).] This figure emphasizes the most important result of our calculations of $\overline{v\theta}$, i.e., in general, the heat transport is poleward near the maxima in the zonal wind and is equatorward near the minima. In all cases the *integrated* flux for $-1\leqslant\alpha\leqslant+1$ is poleward. Also, we note that the zonal average of v_2 is identically zero for geostrophic motion, and therefore any contribution to the meridional heat transport by the mean

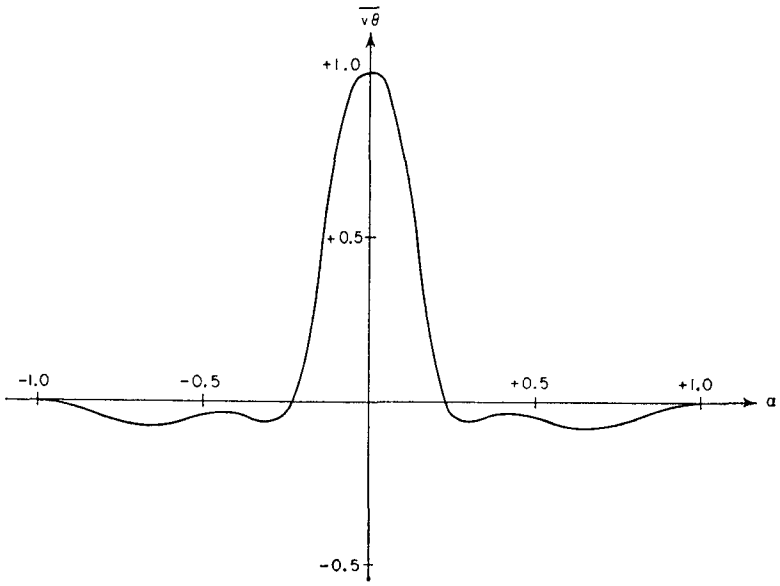

FIG. 4. As in Fig. 1, but for $\bar{u}=(1+\alpha^2)^{-1}$.

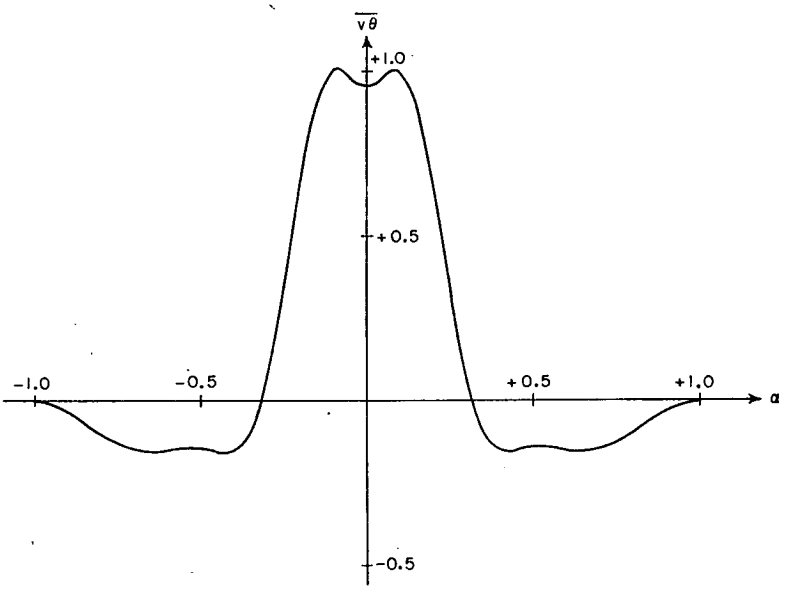

FIG. 5. As in Fig. 1, but for $\bar{u}=(1+\alpha^2)^{-1}$ and $b=3.65$.

motions generated by baroclinic waves is small compared to the eddy transport.

The equatorward transport of heat by eddies near minima in $\bar{u}$ is also apparent in observations of the atmosphere. For example, Oort and Rasmusson's data (1971, Fig. 23) show that the eddy transport between the equator and about 20N is typically toward the equator. The magnitude of this transport is not as large as in Figs. 1–7, because the real atmosphere is a lot farther from neutral stability than the solutions used in our calculations (cf. the trend in Figs. 4–6). Observations north of 75N are not adequate for determining if equatorward transports also occur in polar regions although there are some hints of such a transport (Oort and Rasmusson, 1971, Fig. E4). Some numerical general circulation models do show equatorward eddy transports in polar regions (Holloway and Manabe, 1971, Fig. 27). Such a transport would supply a positive feedback to the mean temperature structure in polar regions, in contrast to the negative feedback in mid-latitudes. The feedback in the eddy fluxes is very strong (Stone, 1973) and a positive feedback in polar regions could have important effects in climatological calculations.

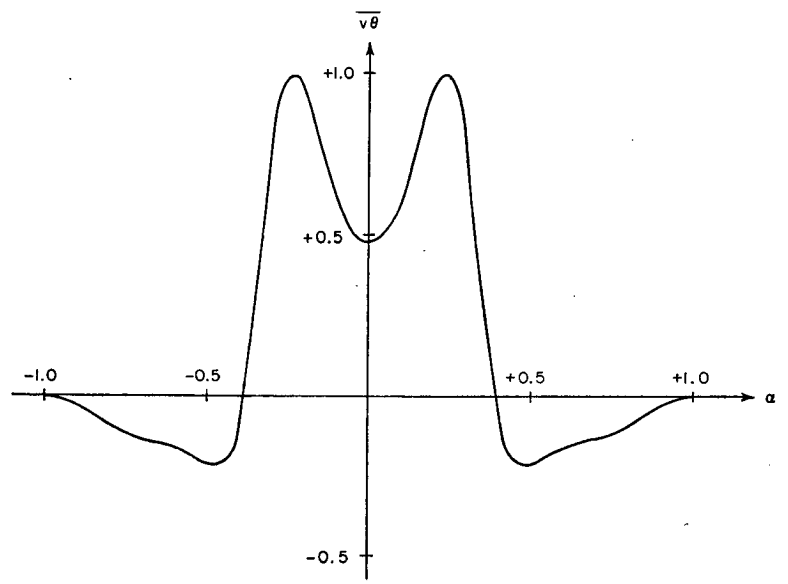

FIG. 6. As in Fig. 1, but for $\bar{u}=(1+\alpha^2)^{-1}$ and $b=3.5$.

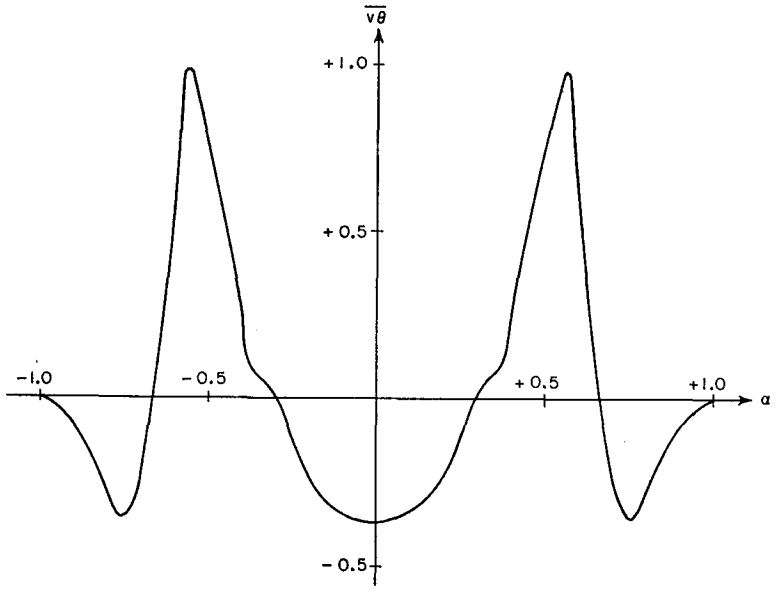

FIG. 7. As in Fig. 1, except that $\bar{u}(y)$ consists of two weak jets, symmetrically placed at $\alpha=\pm\frac{1}{2}$.

These equatorward transports can be easily explained. From Eqs. (2.6), (2.7) and (2.17) we have

$$\overline{\theta v}=-kg_i\left|\frac{\sin\eta}{[\lambda(1+g^2)]^{\frac{1}{2}}}\right|^2. \tag{3.2}$$

Thus, the sign of $\overline{v\theta}$ is determined by g. Since g depends on the *local* value of u, i.e., the local baroclinicity, the direction of $\overline{\theta v}$ is completely determined by the local value of $\bar{u}$. This is characteristic of problems in which a "two-timing" approximation is appropriate; the correlations are primarily dependent on the modulations associated with the slowly varying functions (in this case $\bar{u}$) rather than those associated with the rapidly varying functions (in this case Π_1 and Π_3). The same behavior occurs in the eddy momentum flux (Stone, 1969). Thus, one would anticipate that to a first approximation the heat flux is equatorward in regions where the *local* criterion for stability is satisfied, and poleward in regions where it is not. If we define b' to be the local value of b, i.e.,

$$b'=\frac{\beta L^2}{u_0\bar{u}(\alpha)}=\frac{b}{\bar{u}(\alpha)}, \tag{3.3}$$

then, since the critical value for instability is $b=4.0$ (Stone, 1969), the locations where the flux changes sign, α_c, will be given by

$$\bar{u}(\alpha_c)=\frac{b}{4.0}. \tag{3.4}$$

This formula should be accurate as long as $\epsilon\ll 1$.

Fig. 8 shows how well the simple formula (3.4) agrees with the detailed calculation of the fluxes from Eqs. (2.6)–(2.17). The solid lines give the values of α_c predicted by Eq. (3.4) and the ×'s indicate the actual values from the calculations of $\overline{v\theta}$. The agreement is

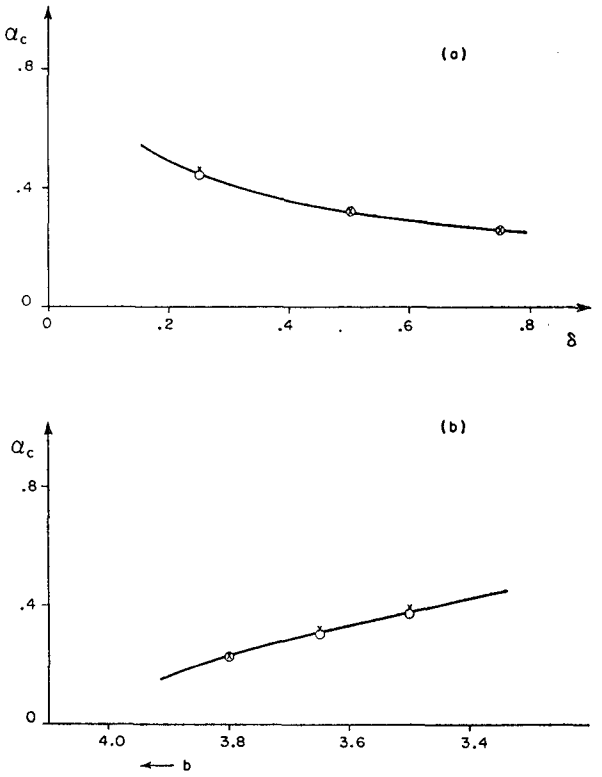

FIG. 8. Comparison of predicted and actual location of the zeros in the fluxes. The curves give the predicted location [Eq. (3.4)], the ×'s the actual locations for $\overline{\theta v}$, and the o's the actual locations for $\overline{\theta w}$. See text for explanation.

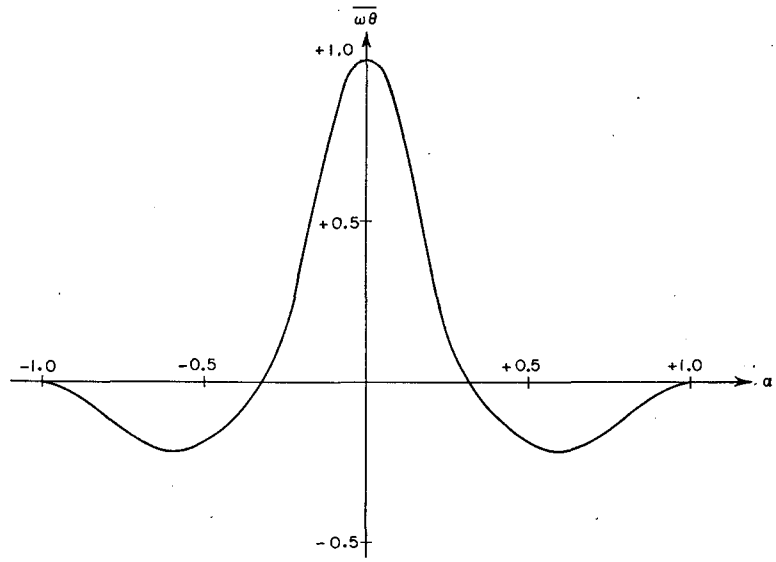

FIG. 9. Vertical heat transport vs latitude for $b=3.8$, $\bar{u}=1-\frac{1}{2}\alpha^2$.

excellent. Fig. 8a gives the values of α_c when $b=3.8$ and $\bar{u}=1-\delta\alpha^2$, and shows how α_c depends on the horizontal shear δ. Fig. 8b gives the values when $u=(1+\alpha^2)^{-1}$, and shows how α_c depends on the vertical shear b. For mean atmospheric conditions, Eq. (3.4) predicts a reversal in the flux at about 20° latitude, which is consistent with the observations (Oort and Rasmusson, 1971, Fig. 23).

4. The vertical eddy heat flux

As one would expect from Eq. (2.19) the distribution of the vertical eddy heat flux and its dependence on b and $\bar{u}$ closely resembles those found in the horizontal flux. Figs. 9–11 suffice to show this resemblence. They show $\overline{w\theta}$, normalized to its maximum value, for the same values of b and $\bar{u}$ used in Figs. 2, 4 and 6, respectively. The vertical transport is positive near maxima in $\bar{u}$, negative near minima in $\bar{u}$, and the regions of positive transport become larger as one moves away from neutral stability. The remarks made in the preceding section about the dependence of $\overline{v\theta}$ on the local value of the baroclinicity apply equally well to $\overline{w\theta}$. In Fig. 8 the O's indicate the location of the zeros in $\overline{w\theta}$ calculated using Eqs. (2.6)–(2.18). Again they are in excellent agreement with the locations predicted by Eq. (3.4).

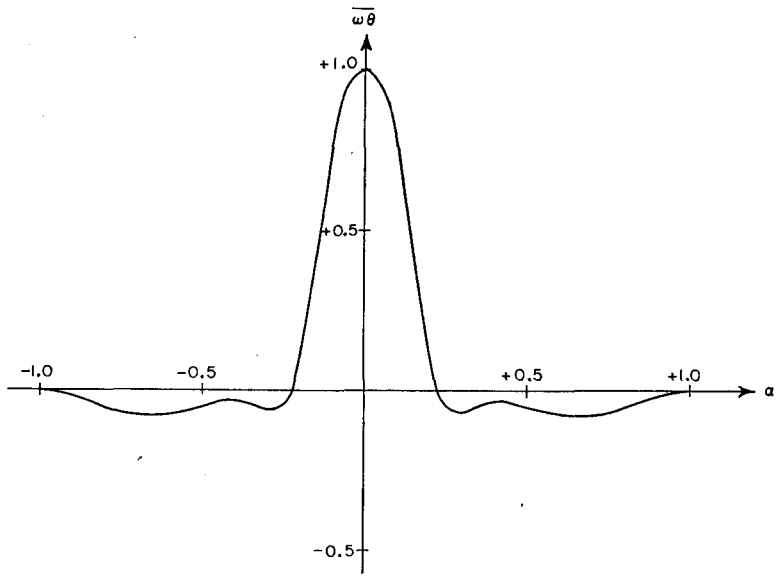

FIG. 10. As in Fig. 9, but for $\bar{u}=(1+\alpha^2)^{-1}$.

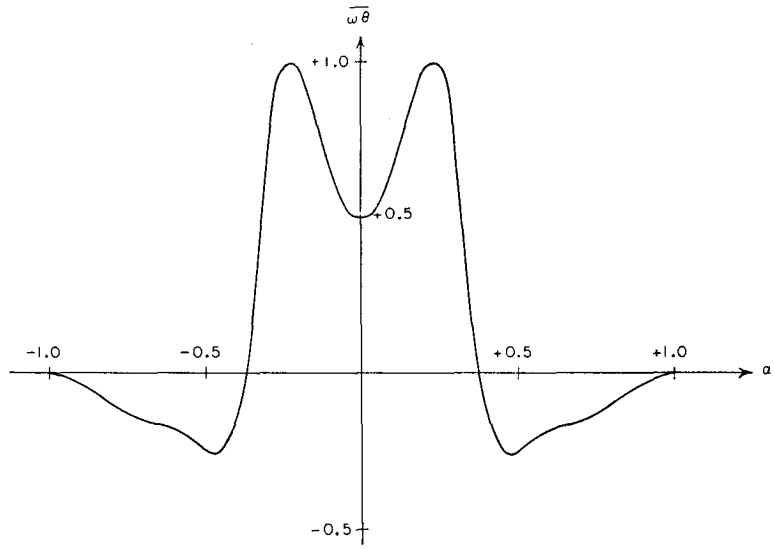

FIG. 11. As in Fig. 9, but for $\bar{u}=(1+\alpha^2)^{-1}$ and $b=3.5$.

Since the vertical motions accompanying the baroclinic wave are of order of the Rossby number, the vertical heat transport due to the mean motions generated by the baroclinic wave are comparable to the eddy transport, $\overline{\theta w}$. However, mass conservation requires that the mean vertical motions integrated latitudinally be zero. Comsequently, the latitudinally averaged vertical heat transport arises solely from the eddy transport, $\overline{\theta v}$. In all cases this integrated transport is upward, as it should be for a growing baroclinic wave.

5. Parameterization of the eddy heat fluxes

We will start from our earlier parameterization for the eddy fluxes (Stone, 1972) but without the *ad hoc* meridional dependence originally introduced. We will also simplify the expressions by assuming that the Richardson number is large compared to unity. The simplified formulas are

$$\overline{\theta v}=-0.144\frac{gH^2}{f^2T}\left(\frac{g}{T}\frac{\partial\bar{\theta}}{\partial z}\right)^{\frac{1}{2}}\left|\frac{\partial\bar{\theta}}{\partial y}\right|\frac{\partial\bar{\theta}}{\partial y}, \tag{5.1}$$

$$\overline{\theta w}=+0.36\frac{g^2H}{f^2T^2}\left(\frac{g}{T}\frac{\partial\bar{\theta}}{\partial z}\right)^{-\frac{1}{2}}\left|\frac{\partial\bar{\theta}}{\partial y}\right|^3 z\left(1-\frac{z}{H}\right), \tag{5.2}$$

where g is the acceleration of gravity, H the scale height, f the Coriolis parameter, T the temperature, and z the height above the ground. These expressions were derived in part by using Eady's (1949) model of baroclinic stability, in which H, f, T, $\partial\bar{\theta}/\partial z$ and $\partial\bar{\theta}/\partial y$ are all constant. Consequently, in our earlier work (Stone, 1972, 1973) f was evaluated at 45° latitude, values of the other quantities averaged over the whole troposphere were used, and an *ad hoc* meridional dependence was introduced. The calculations in Sections 2–4 allowed for meridional variations in $\partial\bar{\theta}/\partial y$ explicitly and for variations in f implicitly through the β-plane approximation. Thus, we can now introduce modifications into Eqs. (5.1) and (5.2) to allow for the variations of $\partial\bar{\theta}/\partial y$ and for the β-effect.

Our calculations showed that it is the local value of $\bar{u}$ that matters, and $\bar{u}$ is related to $\partial\bar{\theta}/\partial y$ by the thermal wind relation for the two-level model:

$$2fu_0\bar{u}=-\frac{g}{T}\frac{\partial\bar{\theta}}{\partial y}. \tag{5.3}$$

Therefore, we will include the meridional variation of $\partial\bar{\theta}/\partial y$ by simply re-interpreting $\partial\bar{\theta}/\partial y$ in Eqs. (5.1) and (5.2). Instead of interpreting it as the mean tropospheric value of $\partial\theta/\partial y$, we will now interpret it as the local value of $\partial\theta/\partial y$ averaged longitudinally and vertically, with the vertical average being a mass-weighted average between the ground and the tropopause. Consequently, $\partial\bar{\theta}/\partial y$ will now be a function of latitude.

The β-effect is measured by the local value of b, given by Eq. (3.3). This local value b' can be written in more convenient form by substituting for $\bar{u}$ from Eq. (5.3) and for L its definition,

$$L=\frac{H}{f}\left(\frac{g}{T}\frac{\partial\bar{\theta}}{\partial z}\right)^{\frac{1}{2}}. \tag{5.4}$$

We obtain

$$b'=-2\beta H\frac{\partial\bar{\theta}}{\partial z}\Big/f\frac{\partial\bar{\theta}}{\partial y}. \tag{5.5}$$

If we evaluate both f and β at 45° latitude then (5.5)

becomes

$$b'=-\frac{2H}{R}\frac{\partial\bar{\theta}/\partial z}{\partial\bar{\theta}/\partial y}. \tag{5.6}$$

This expression shows that b' is essentially a measure of the local slope of the isentropes. The critical value $b'=4$ corresponds to a slope equal to $\frac{1}{2}H/R$. If there were no β-effect, the critical slope would be zero. This result suggests that the β-effect may be included in our parameterization by introducing a critical slope for the isentropes.

To implement this idea, it is convenient to use the formalism introduced by Reed and German (1965). They write the eddy transports in the form

$$\overline{\theta v}=-K\left(\frac{\partial\bar{\theta}}{\partial y}+\bar{\gamma}\frac{\partial\bar{\theta}}{\partial z}\right), \tag{5.7}$$

$$\overline{\theta w}=-K\left[\bar{\gamma}\frac{\partial\bar{\theta}}{\partial y}+(\bar{\gamma}^2+\overline{\gamma'^2})\frac{\partial\bar{\theta}}{\partial z}\right], \tag{5.8}$$

where K is an eddy diffusivity, $\bar{\gamma}$ the mean slope of the mixing surfaces in the meridional plane, and $\overline{\gamma'^2}$ the mean-square standard deviation of the slope. Analogous expressions describe the eddy transports for any conservative quantity. Green (1970) used a similar formulation for the eddy transports of heat by large-scale eddies, but he implicitly assumed that $\overline{\gamma'^2}\gg\bar{\gamma}^2$. This assumption can be rationalized if the large-scale eddies which cause mixing do indeed arise from baroclinic instability. Stability theory indicates that one particular slope is favored for the mixing surfaces, and other slopes cannot compete effectively because of the exponential differential growth of the eddies with different mixing slopes. This implies that $\overline{\gamma'^2}\ll\bar{\gamma}^2$. The same conclusion is suggested by the sharp peak in atmospheric wavenumber spectra of the meridional velocity (Kao and Wendell, 1970). In any case we too will assume that the eddies are generated in such a way that $\overline{\gamma'^2}\ll\bar{\gamma}^2$.

With this assumption $\bar{\gamma}$ and K can be found from any parameterization for $\overline{v\theta}$ and $\overline{w\theta}$, and used to describe the eddy diffusion of any conservative property. From Eqs. (5.7) and (5.8) we have

$$\bar{\gamma}=\frac{\overline{\theta w}}{\overline{\theta v}}. \tag{5.9}$$

Substituting from Eqs. (5.1) and (5.2), we find

$$\bar{\gamma}=-\frac{5}{2}\frac{z}{H}\left(1-\frac{z}{H}\right)\frac{\partial\bar{\theta}/\partial y}{\partial\bar{\theta}/\partial z}. \tag{5.10}$$

This is the mixing slope predicted by Eady's model, in the long-wave limit. It has a maximum equal to $\frac{5}{8}$ of the isentropic slope, and it goes to zero at the top and bottom of Eady's Boussinesq atmosphere, because of the rigid boundaries placed there. It would be more realistic to place the upper rigid boundary at the tropopause than one scale height above the ground, so we will replace H in Eq. (5.10) by z_T, the height of the tropopause. Substituting Eqs. (5.10) and (5.1) into (5.7), we find

$$K=0.144gH^2\left(\frac{g}{T}\frac{\partial\bar{\theta}}{\partial z}\right)^{\frac{1}{2}}\left|\frac{\partial\bar{\theta}}{\partial y}\right|\Big/f^2T\left[1-\frac{5}{2}\frac{z}{z_T}\left(1-\frac{z}{z_T}\right)\right]. \tag{5.11}$$

Since the slope of the isentropes directly determines $\bar{\gamma}$, but not K, we will introduce the critical isentropic slope by modifying $\bar{\gamma}$. In particular, we will replace (5.10) by

$$\bar{\gamma}=-\frac{5}{2}\frac{z}{z_T}\left(1-\frac{z}{z_T}\right)\frac{\partial\bar{\theta}/\partial y}{\partial\bar{\theta}/\partial z}F(b'), \tag{5.12}$$

and choose $F(b')$ to satisfy the following criteria:

1) $F(0)=1$, so $\bar{\gamma}$ reduces to the form derived using Eady's model when $\beta=0$.

2) $\int_0^{z_T}\overline{v\theta}dz=0$ when $b'=4$, so that the mean fluxes change sign at the critical isentropic slope determined from the two-layer model.

3) F is a symmetric function of b', since the stability of the zonal flow does not depend on the sign of b'.

The simplest function satisfying these criteria is

$$F(b')=1+0.283|b'|. \tag{5.13}$$

Substituting (5.13) and (5.6) into (5.12), we find for the modified mixing slope

$$\bar{\gamma}=-\left[\frac{5}{2}\frac{\partial\bar{\theta}/\partial y}{\partial\bar{\theta}/\partial z}+1.42\frac{H}{R}\frac{\partial\bar{\theta}/\partial y}{|\partial\bar{\theta}/\partial y|}\right]\frac{z}{z_T}\left(1-\frac{z}{z_T}\right). \tag{5.14}$$

The modified form of the meridional flux is now found by substituting (5.11) and (5.14) into (5.7). We obtain

$$\overline{\theta v}=\frac{-0.144gH^2}{f^2T}\left(\frac{g}{T}\frac{\partial\bar{\theta}}{\partial z}\right)^{\frac{1}{2}}\times\frac{\partial\bar{\theta}}{\partial y}\left[\left|\frac{\partial\bar{\theta}}{\partial y}\right|-\frac{1.42\dfrac{z}{z_T}\left(1-\dfrac{z}{z_T}\right)}{1-\dfrac{5}{2}\dfrac{z}{z_T}\left(1-\dfrac{z}{z_T}\right)}\frac{H}{R}\frac{\partial\bar{\theta}}{\partial z}\right]. \tag{5.15}$$

Eq. (5.15) can be put in a computationally simpler form if we: 1) substitute for H its definition,

$$H=\frac{R_0T}{g}, \tag{5.16}$$

where R_0 is the gas constant; 2) replace $\partial\bar{\theta}/\partial z$ by the

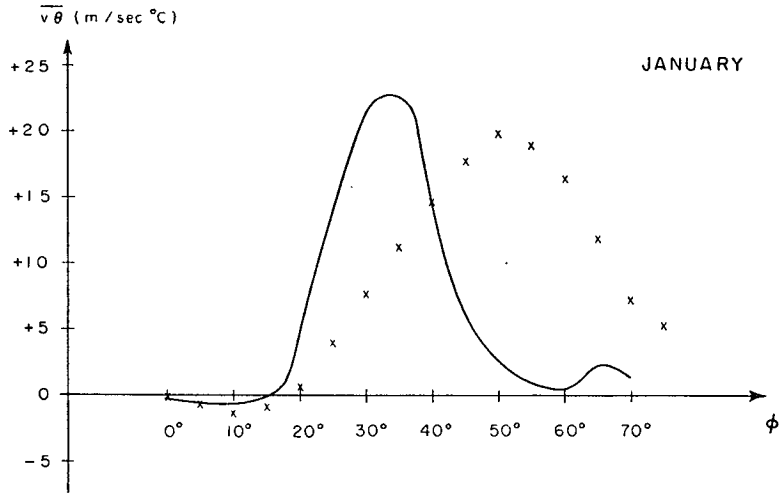

FIG. 12. Tropospheric meridional eddy flux for January. The ×'s indicate Oort and Rasmusson's (1971) data.

derivative of $\bar{\theta}$ with respect to the pressure p assuming hydrostatic equilibrium and a perfect gas,

$$\frac{\partial\bar{\theta}}{\partial z}=-\frac{p}{H}\frac{\partial\bar{\theta}}{\partial p}; \tag{5.17}$$

and 3) replace $\partial\bar{\theta}/\partial y$ by the latitudinal gradient,

$$\frac{\partial\bar{\theta}}{\partial y}=\frac{1}{R}\frac{\partial\bar{\theta}}{\partial\phi}. \tag{5.18}$$

Eq. (5.15) then becomes

$$\overline{\theta v}=-0.144\frac{R_0^{\frac{2}{3}}}{R^2f^2}\left(p\left|\frac{\partial\theta}{\partial p}\right|\right)^{\frac{1}{3}}\left[\left|\frac{\partial\bar{\theta}}{\partial\phi}\right|+h(z)p\frac{\partial\theta}{\partial p}\right], \tag{5.19}$$

where

$$h(z)=1.42\frac{x(1-x)}{1-\frac{5}{2}x(1-x)},\quad x=\frac{z}{z_T}. \tag{5.20}$$

In (5.19) R_0, R and f are all constants; $\overline{p(\partial\theta/\partial p)}$ is still taken to be the mass-weighted tropospheric value of $\overline{p(\partial\theta/\partial p)}$ (neither Eady's model nor the two-level model allow variations in the static stability); $\partial\bar{\theta}/\partial\phi$ is now a function of latitude only; and h is a function of height and of latitude (through z_T).

In order to check the validity of Eq. (5.19) we used it to calculate $\overline{\theta v}$ from the distributions of $\bar{\theta}$ given by Oort and Rasmusson (1971) for the Northern Hemisphere. The following values for the constants were adopted: $R_0=2.9\times10^6$ ergs $(°K)^{-1}$ gm^{-1}, $R=6370$ km, and f (at 45° latitude) $=1.03\times10^{-4}$ sec^{-1}. The meridional flux calculated from the mean January distribution of $\bar{\theta}$ is illustrated in Fig. 12. This figure shows the vertically averaged (mass-weighted) values of $\overline{\theta v}$ for the troposphere as a function of latitude. The mass-weighted tropospheric value of $\overline{p(\partial\theta/\partial p)}$ was −36C. Observational values of $\overline{\theta v}$ averaged in the same way were calculated from Oort and Rasmusson's (1971) data for the eddy transports of sensible heat and potential energy. These observed values are shown as ×'s in Fig. 12 and in all subsequent figures. The parameterization gives reasonably accurate values for the flux maximum and for the latitude of the reversal in the flux in low latitudes. However, the flux maximum is located 15° too far south. In the parameterization this maximum is always located where the horizontal temperature gradient is a maximum. Evidently in the atmosphere the maximum in the flux is not tied so closely to the maximum in the temperature gradient.

Fig. 13 illustrates the vertical dependence of the meridional flux at 40N in January calculated from (5.19). The vertical dependence agrees reasonably well with the observations, showing two maxima in the flux, one near the ground and one near the tropopause. Apparently this double maximum can be explained by the leveling-off of the mixing surfaces near the ground and the tropopause [cf. Eq. (5.14)]. The parameterization misses the decrease of the flux in the boundary layer, because the boundary layer was neglected in both of the stability models used in deriving the parameterization. Also the parameterization gives poor results in the stratosphere. This defect can be traced to the neglect of the vertical variations of baroclinicity and static stability in both Eady's model and the two-level model.

The parameterization can also be compared with the horizontal eddy fluxes found in three-dimensional general circulation models (GCM's). Three groups of investigators have used GCM's for simulating January conditions, and have published values of the meridional eddy flux of sensible heat generated by their models—

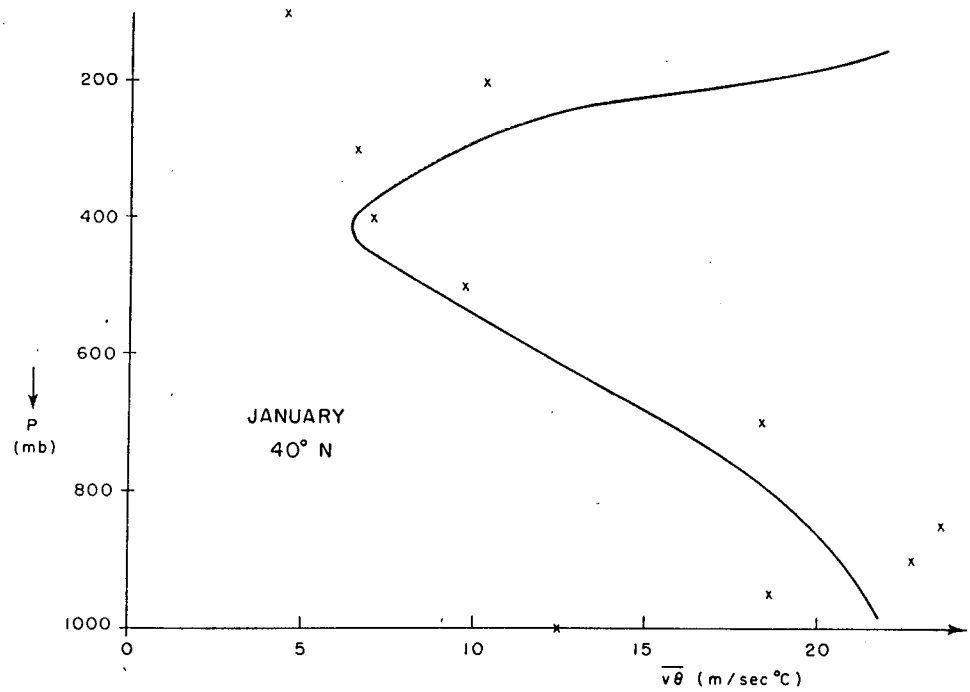

FIG. 13. Meridional flux as a function of pressure at 40N in January. The X's indicate Oort and Rasmusson's data.

the GFDL group (Holloway and Manabe, 1971, Fig. 27), the GISS group (Sommerville *et al.*, 1974, Fig. 26), and the NCAR group (Kasahara *et al.*, 1973, Fig. 10). The NCAR calculations used a 12-level model, while the GFDL and GISS calculations used 9-level models. The GCM's and the parameterization give comparable results for the locations of the flux reversal and the double maximum in the poleward flux, but the GCM's do better in locating the flux maximum. They all locate it at about 45N, only 5° south of the observed location. The one factor that is included in all the GCM's but not in the stability analyses used as the basis for the parameterization which could plausibly account for this difference is curvature effects. Table 1 compares the maximum values for the meridional flux in January given by the different models. Again the GCM's and the parameterization give comparable results. The error quoted for the observed maximum corresponds to the standard deviation arising from inter-annual variations [see Fig. E4 of Oort and Rasmusson (1971)].

The vertically averaged values of $\overline{\theta v}$ calculated from Eq. (5.19) for July mean values of $\bar{\theta}$ are shown in Fig.

TABLE 1. Comparison of maximum values of January meridional heat flux $\overline{v\theta}$.

Model	Relative value
Observed	1.0±0.1
GFDL	0.9
GISS	0.7
NCAR	0.7
Eq. (5.19)	1.1

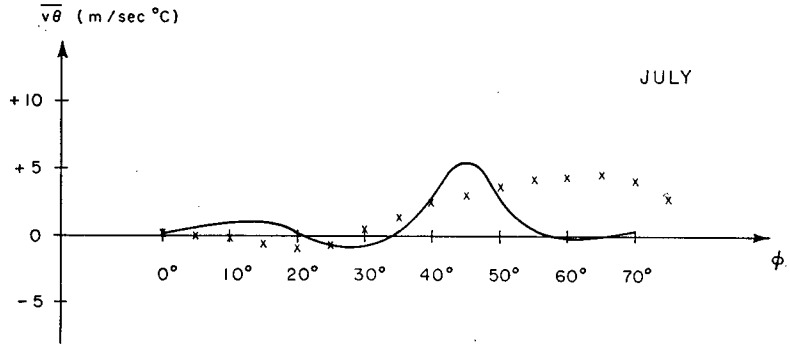

FIG. 14. As in Fig. 12, but for July.

14, together with Oort and Rasmusson's observed values. The vertical variations in July are illustrated in Fig. 15. For July the mass-weighted tropospheric value of $\overline{p(\partial\theta/\partial p)}$ was −38C. The small seasonal variability of this quantity and the small changes in it found in our earlier investigation of the effects of climatic change (Stone, 1973) indicate that this quantity may be taken to be a constant for most purposes. The July observations do not provide as good a check of the parameterization as the January observations, since the standard deviation in the observations is larger in July than in January. Nevertheless, the July comparison essentially verifies the conclusions reached about the parameterization from the January comparison. Most importantly, the parameterization reproduces accurately the seasonal change in the magnitude of the flux.

The vertical eddy flux $\overline{\theta w}$ is obtained by multiplying $\bar{\gamma}$ [Eq. (5.14)], by $\overline{\theta v}$ [Eq. (5.15)]. Since there are no observations of the vertical eddy flux available, it is not possible to check this parameterization the way we checked that for the meridional flux. Previously (Stone, 1973) we showed that the magnitude of the vertical flux predicted by Eq. (5.2) agrees with Palmén and Newton's (1969) rough estimate of the flux in winter north of 32° latitude. This rough check also holds for values of the flux calculated using the modified form of $\bar{\gamma}$ since in winter north of 32° the modifications we introduced are not large.

Finally, it is worth pointing out that the viability of our parameterization is not strongly dependent on the mechanistic approach we used to derive it. There are two crucial assumptions involved (cf. Stone, 1972). The first is that the slope of the mixing surfaces are given correctly by baroclinic stability theory. These slopes are likely to be correct even if the eddies are not generated by baroclinic instability, since they represent the slopes along which it is easiest for displacements to occur—i.e., the slopes along which a minimum amount of work is done against gravity. The second assumption is that the growth of the eddies is limited by nonlinear effects, so that there is an equipartition between the mean zonal kinetic energy and the total eddy kinetic energy. This assumption can hold regardless of how the eddies arise. In fact, in winter months the dominant contribution to the total eddy flux is by the stationary eddies (Oort and Rasmusson, 1971, Tables C7a and C7b), and these probably arise from topographical and diabatic heating effects rather than from baroclinic instability (Derome and Wiin-Nielsen, 1971). Nevertheless, our parameterization gave good results for the total eddy transport in January.

6. Summary

The calculations of the eddy fluxes of sensible heat in Sections 3 and 4 show the importance of local baroclinicity in determining the direction of the fluxes. In

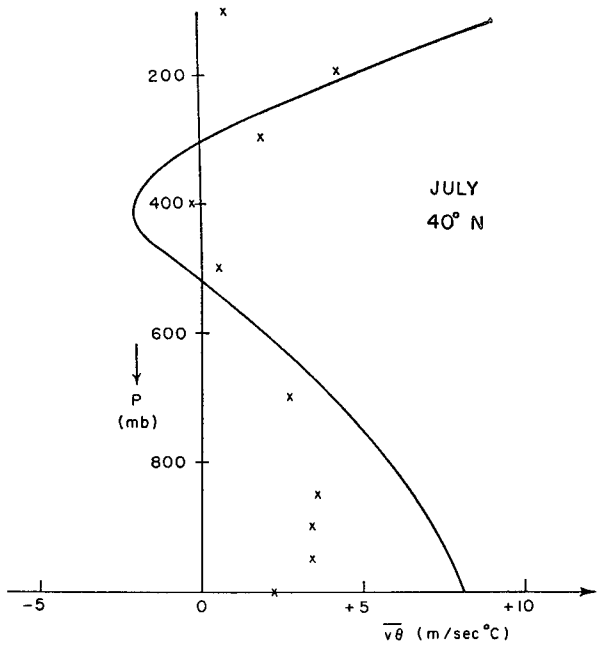

FIG. 15. As in Fig. 13, but for July.

regions where $b'<4$ the slope of the isentropes exceeds the critical value and heat is transported poleward and upward. In regions where $b'>4$ the slope of the isentropes is less than the critical value and heat is transported equatorward and downward. This result agrees with the observed reversal in the meridional eddy flux in low latitudes. Observations in high latitudes are not yet adequate for determining whether a similar reversal occurs there. The existence of such a reversal would have important climatological implications. It would mean that the negative feedback between the mean temperature field and the eddy fluxes in mid-latitudes becomes a positive feedback in high latitudes, and the polar regions would be more susceptible to climatic change on this account.

The comparison between the eddy flux parameterization and the observations in Section 5 indicates that it is feasible to use zonal average models with parameterizations of the eddy processes in order to study climatological problems. In particular, using the parameterizations of the eddy sensible heat fluxes presented in Section 5, one can model the magnitude and sign of the tropospheric fluxes and their vertical variations and seasonal changes. The eddy fluxes of other conservative quantities can be modeled with comparable accuracy by using the same values for the eddy diffusion coefficient and the slope of the mixing surface. The meridional eddy flux of momentum can be calculated from the fluxes of sensible heat and potential vorticity by using Green's (1970) prescription.

The one notable defect in the parameterization is the location of the maximum poleward flux. An analysis of the baroclinic stability problem with curvature

effects included might supply the insight necessary to correct this defect. It also might be possible to extend the parameterization to the stratosphere by analyzing a model of baroclinic stability which included vertical variations in the baroclinicity and the static stability.

Acknowledgments. I am indebted to Mr. Richard Tzong for carrying out most of the numerical calculations reported in Sections 3 and 4. This work was supported in part by the Atmospheric Sciences Program of the National Science Foundation under Grant GA 28371 to Harvard University.

REFERENCES

Charney, J. G., and N. A. Phillips, 1953: Numerical integration of the quasigeostrophic equations of motion for barotropic and simple baroclinic flows. *J. Meteor.*, **10**, 71–99.

Clapp, P. F., 1970: Parameterization of macroscale transient heat transport for use in a mean motion model of the general circulation. *J. Appl. Meteor.*, **9**, 554–563.

Derome, J., and A. Wiin-Nielsen, 1971: The response of a middle-latitude model atmosphere to forcing by topography and stationary heat sources. *Mon. Wea. Rev.*, **99**, 564–576.

Eady, E. T., 1949: Long waves and cyclone waves. *Tellus*, **1**, No. 3, 33–52.

Green, J. S. A., 1970: Transfer properties of the large-scale eddies and the general circulation of the atmosphere. *Quart. J. Roy. Meteor. Soc.*, **96**, 157–185.

Holloway, J. L., and S. Manabe, 1971: Simulation of climate by a global general circulation model. 1. Hydrologic cycle and heat balance. *Mon. Wea. Rev.*, **99**, 335–370.

Kao, S-K., and L. Wendell, 1970: The kinetic energy of the large-scale atmospheric motions in wavenumber-frequency space. *J. Atmos. Sci.*, **27**, 359–375.

Kasahara, A., T. Sasamori and W. M. Washington, 1973: Simulation experiments with a 12-layer stratospheric global circulation model. Part I. *J. Atmos. Sci.*, **30**, 1229–1251.

Kuo, H.-L., 1956: Forced and free meridional circulations in the atmosphere. *J. Meteor.*, **13**, 561–568.

Kurihara, Y., 1970: A statistical-dynamical model of the general circulation of the atmosphere. *J. Atmos. Sci.*, **27**, 847–870.

Oort, A. H., and E. Rasmusson, 1971: Atmospheric circulation statistics. NOAA Prof. Paper 5, 323 pp.

Palmén, E., and C. W. Newton, 1969: *Atmospheric Circulation Systems*. New York, Academic Press, 603 pp.

Phillips, N. A., 1954: Energy transformations and meridional circulations associated with simple baroclinic waves in a two-level, quasi-geostrophic model. *Tellus*, **6**, 273–286.

Reed, R. J., and K. E. German, 1965: A contribution to the problem of stratospheric diffusion by large-scale mixing. *Mon. Wea. Rev.*, **93**, 313–321.

Saltzman, B., and A. D. Vernekar, 1971: An equilibrium solution for the axially symmetric component of the earth's macroclimate. *J. Geophys. Res.*, **76**, 1498–1524.

Sellers, W. D., 1969: A global climatic model based on the energy balance of the earth-atmosphere system. *J. Appl. Meteor.*, **8**, 392–400.

Somerville, R. C. J., P. H. Stone, M. Halem, J. E. Hansen, J. S. Hogan, L. M. Druyan, G. Russell, A. Lacis, W. Quirk and J. Tenenbaum, 1974: The GISS model of the global atmosphere. *J. Atmos. Sci.*, **31**, 84–117.

Stone, P. H., 1969: The meridional structure of baroclinic waves. *J. Atmos. Sci.*, **26**, 376–389.

——, 1972: A simplified radiative-dynamical model for the static stability of rotating atmospheres. *J. Atmos. Sci.*, **29**, 405–418.

——, 1973: The effect of large scale eddies on climatic change. *J. Atmos. Sci.*, **30**, 521–529.

Wiin-Nielsen, A., 1970: A theoretical study of the annual variation of the atmospheric energy. *Tellus*, **22**, 1–16.